

## Research Article

Giulia Fredi\*, Andrea Dorigato, Luca Fambri, José-Marie Lopez-Cuesta, and Alessandro Pegoretti

# Synergistic effects of metal hydroxides and fumed nanosilica as fire retardants for polyethylene

<https://doi.org/10.1515/flret-2019-0004>

Received Jun 22, 2018; revised Aug 24, 2018; accepted Aug 27, 2018

**Abstract:** This work aims to study the synergistic effect of aluminum/magnesium hydroxide microfillers and organomodified fumed silica nanoparticles as flame retardants (FRs) for linear low-density polyethylene (LLDPE), and to select the best composition to produce a fire-resistant polyethylene-based single-polymer composite. The fillers were added to LLDPE at different concentrations, and the prepared composites were characterized to investigate the individual and combined effects of the fillers on the thermo-oxidation resistance and the fire performance, as well as the microstructural, physical, thermal and mechanical properties. Both filler types were homogeneously distributed in the matrix, with the formation of a network of silica nanoparticles at elevated loadings. Melt flow index (MFI) tests revealed that the fluidity of the material was not considerably impaired upon metal hydroxide introduction, while a heavy reduction of the MFI was detected for silica contents higher than 5 wt%. FRs introduction promoted a noticeable enhancement of the thermo-oxidative stability of the materials, as shown by thermogravimetric analysis (TGA) and onset oxidation temperature (OOT) tests, and superior thermal properties were measured on the samples combining micro- and nanofillers, thus evidencing synergistic effects. Tensile tests showed that the stiffening effect due to a high content of metal hydroxide microparticles was accompanied by a decrease in the strain at break, but nanosil-

ica at low concentration contributed to preserve the ultimate mechanical properties of the neat polymer. The fire performance of the samples with optimized compositions, evaluated through limiting oxygen index (LOI) and cone calorimetry tests, was strongly enhanced with respect to that of the neat LLDPE, and also these tests highlighted the synergistic effect between micro- and nanofillers, as well as an interesting correlation between fire parameters and viscosity.

**Keywords:** fumed silica, polyethylene, nanocomposites, fire retardants, cone calorimetry

## 1 Introduction

The massive employment of polymers and polymer-matrix composites has been driven by their combination of low density, high processability and interesting mechanical and physical properties [1, 2]. Polyolefins, and polyethylene (PE) in particular, are among the most widely used thermoplastic polymers, due to the remarkable combination of high chemical resistance, good mechanical properties and cheapness. Among the classes of PE, linear low-density polyethylene (LLDPE) has emerged for high impact and tear strength and film-drawing tendencies, which widen the range of applications of this polymer in the film and packaging industry [1, 3, 4]. One of the major drawbacks of polymers and polymer composites is represented by their high flammability, and thus the improvement of flame resistance of polymers is crucial to broaden their use and meet the increasingly stringent safety requirements [2, 5, 6].

To reach this goal, the most common approach is to add flame retardants (FRs). Depending on their nature, FRs operate physically and/or chemically in the solid, liquid or gas phase and hinder combustion at different levels [7].

There are many types of FRs, which can be classified according to their chemistry, morphology or FR mechanism. The most common are metal hydroxides, boron-based FRs, halogen-based FRs, phosphorous-based FRs,

**\*Corresponding Author: Giulia Fredi:** University of Trento, Department of Industrial Engineering and INSTM research unit Via Sommarive 9 – 38123 Trento, Italy; Email: giulia.fredi@unitn.it; Tel. +39 0461/282539

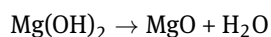
**Andrea Dorigato, Luca Fambri:** University of Trento, Department of Industrial Engineering and INSTM research unit Via Sommarive 9 – 38123 Trento, Italy

**José-Marie Lopez-Cuesta:** Ecole des Mines d'Alés (CMGD), 6, Avenue de Clavières, 30319 Cedex, Alés, France

**Alessandro Pegoretti:** University of Trento, Department of Industrial Engineering and INSTM research unit Via Sommarive 9 – 38123 Trento, Italy; Email: alessandro.pegoretti@unitn.it; Tel. +39 0461/282452

silicon-based FRs, nitrogen-based FRs, intumescent fillers, and nanometric particles [6]. Due to the well known tendency of halogenated FRs to release toxic and corrosive by-products, a significant research activity has focused on halogen-free FRs, in order to find less hazardous and more environmentally friendly alternatives [6–10].

One of the most diffused classes of halogen-free FRs is represented by the metal hydroxides [11, 12]. These FRs, normally provided in the form of micrometric particles, are generally used in high weight fractions, also up to 70 wt%. In this way, they act as a solid phase diluent and reduce the rate of oxygen diffusion into the polymer bulk, while enhancing the heat capacity, thermal conductivity and emissivity [13]. At a specific temperature, normally close to the polymer pyrolysis temperature, metal hydroxide FRs are subjected to an endothermic decomposition and act as “heat sinks”, thereby leading to a temperature decrease and slowing down the thermal degradation [14]. To be effective as flame retardants, their decomposition temperature must be higher than the polymer processing temperature and near or slightly below the polymer decomposition temperature. Their decomposition produces metal oxides, water and other inert gases. These gases help in diluting the combustible gas mixture, thus limiting the reagents concentration in the gas phase and consequently the probability of ignition, and water also brings a beneficial cooling effect in the solid and gas phases. The produced metal oxides, besides increasing the average heat capacity, may accumulate on the burning surface creating a protective barrier layer, which physically separates the oxygen from the combustible gases and can act as a smoke suppressant [7, 13–16]. Therefore, metal hydroxide FRs act through three physical mechanisms: (a) the endothermic decomposition, which subtracts heat, (b) the production of diluent inert gases, which decrease the fuel concentration in the gaseous phase, and (c) the accumulation of an inert layer on the polymer surface, which acts as oxygen/fuel barrier [13]. Among the most common metal hydroxide FRs are the aluminum trihydroxide  $\text{Al}(\text{OH})_3$  and the magnesium hydroxide  $\text{Mg}(\text{OH})_2$ . Their decomposition reactions are reported hereafter:



From these reactions, the theoretical loss of water can be calculated as 34.6 wt% for  $\text{Al}(\text{OH})_3$  and 30.9 wt% for  $\text{Mg}(\text{OH})_2$ . Their total decomposition enthalpies are 1300 and 1450 J/g, respectively [17]. The flame retardant effects of aluminum and magnesium hydroxides on polyolefins have been widely investigated [12, 14, 18–22]. One of the major drawbacks of the metal hydroxide FRs is the high

filler loading required to increase the flame resistance significantly, even up to 70 wt%. This can have remarkable effects on the density of the final product, but also on the processability and the mechanical properties, especially the ductility, since a high filler content can lead to an embrittlement of the polymer matrix [14]. One of the possible solutions is to substitute part of the metal hydroxide with another filler having a different chemistry and/or morphology and exploiting another FR mechanism. If the employed FRs act synergistically, the same flame resistance can be achieved with a lower FR amount, which reduces the cost and limits the undesired side effects of FRs [6].

Some researchers have attempted to exploit the FR synergy to reduce the metal hydroxide content. Yen *et al.* [23] studied the effect of aluminum hydroxide and nanoclay on the fire performance of ethylene-propylene-diene monomer (EPDM) rubber. The substitution of a part of aluminum hydroxide with nanoclay was proved effective to increase the resistance to the thermo-oxidative degradation and the limiting oxygen index (LOI) value, and in reducing the peak heat-release rate (pHRR) and the maximal smoke density. The effectiveness of clays has also been highlighted by Liu *et al.* [24], who studied the combined effect of  $\text{Mg}(\text{OH})_2$  and organomodified montmorillonite on the flame resistance of low-density and crosslinked PE; again, the combination of the two FRs resulted in better fire performances with a lower FR amount. Similar studies were carried out using organomodified montmorillonite in substitution of magnesium hydroxide or hydromagnesite in EVA [25] or in LDPE/EVA blends [26].

Regarding other types of synergists, in the work by Sabet *et al.* [27] the flame performance properties of ethylenevinyl acetate (EVA) were enhanced by the incorporation of magnesium/aluminum hydroxides and zinc borate. It was found that a substitution of 5 wt% of metal hydroxide with zinc borate, in a 40:60 EVA:metal hydroxide formulation, led to significant improvements in flame retardancy as measured by LOI, UL-94, and cone calorimetry experiments. The advantage of substituting part of magnesium hydroxide with zinc borate in EVA was also proved in the work by Durin-France *et al.* [28]. Pan *et al.* [22] investigated the influence of fullerene ( $\text{C}_{60}$ ) on the fire performance properties of high-density polyethylene (HDPE)/aluminum hydroxide composites, and observed that a  $\text{C}_{60}$  content of 2% was sufficient to enhance the flame and thermo-oxidative degradation resistance, thus reducing the metal hydroxide content necessary to have a satisfactory fire performance. In both cases, synergistic effects on flame retardancy were highlighted for a total filler loading of 60 wt.%.

From these examples, it is clear that the most widely used flame retardants synergists (co-FRs) are the nanofillers. In fact, nanometric particles, when properly dispersed in polymer matrices, are a versatile filler, known to contribute to a wide range of properties, such as the mechanical, thermal and optical properties, but also the dimensional stability, abrasion resistance, and fire performance [29]. It has been reported that even a low amount of nanofillers can decrease the heat-release rate, due to the formation of a tortuous diffusion path that hinders the gases diffusion in the condensed phases (barrier effect), the tendency to accumulate at the burning interface creating a protective layer and reinforcing the char [29] and also for organomodified montmorillonites the possibility to migrate towards the surface due to viscosity and surface tension gradients [30–32].

Among the nanofillers used as FRs, natural or fumed silica has been investigated either alone or in combination with other flame retardants [33–38]. Cavodeau *et al.* [33] have highlighted synergistic effects between aluminum trihydroxide and diatomite, a natural silica. The authors observed the formation of an expanded layer during cone calorimetry tests and the modification of the melt viscosity of the sample was suggested to explain the reduction in heat-release rate (HRR). Qian *et al.* [34] investigated the combined effect of fumed silica and oil sludge in an EVA matrix and found that the silica addition lowered the HRR, promoted the formation of a denser char layer and helped in smoke suppression. The flame retardant and smoke suppression properties of fumed silica were also studied by Chen *et al.* [35], who observed the improvement in the fire performance and a decrease in total smoke release in thermoplastic polyurethanes filled with an ammonium polyphosphate FR.

Although many efforts have been made on the investigation of the effect of FRs on the fire performance and the resistance to thermo-oxidative degradation of polymers, only in a few works the corresponding mechanical and physical properties are concurrently investigated. Moreover, although the synergistic effect of nanoparticles and other FRs has been investigated to some extent, only few works can be found on the evaluation of the flame retardancy enhancement given by the combination of metal hydroxides and isodimensional fillers, such as fumed silica nanoparticles, even though they have been proven effective in enhancing the mechanical properties and the fire performance of polymers [3, 39, 40].

Based on these considerations, the aim of this work is to study the combined and synergistic effect of aluminum/magnesium hydroxides and fumed silica on the physical properties of LLDPE. A wide range of composi-

tions were investigated, to determine the separate and combined effects of the FRs, and the blends were subjected to a thorough and systematic characterization to take into account not only the flame resistance and the thermal degradation behavior, but also the microstructural, thermal and mechanical properties, as well as the effect of the fillers on the processability and the melt viscosity. The targeted applications of these materials are matrices for PE-based singlepolymer composites (SPC) reinforced with ultrahigh molecular weight polyethylene (UHMWPE) fibers. This paper focuses on the optimization of the properties of the flame-resistant matrix, while the production and characterization of the SPCs will be the subject of a separate report [41].

## 2 Materials and methods

### 2.1 Materials

The linear low-density polyethylene (LLDPE) Flexirene<sup>®</sup> CL10 (density = 0.918 g/cm<sup>3</sup>, melting temperature = 121°C, melt density at 190°C = 0.765 g/cm<sup>3</sup>) was purchased from Versalis SpA (Milan, Italy) in form of granules. It contains antioxidants that make it suitable to produce films with high optical properties. Two metal hydroxide flame retardants were investigated; the aluminum hydroxide Al(OH)<sub>3</sub>Alufy<sup>®</sup> 2 (AF), and the magnesium hydroxide Mg(OH)<sub>2</sub>Hydrofy<sup>®</sup> G1.5 (HF). Both AF and HF were provided in form of micrometric particles by Nuova Sima Srl (Ancona, Italy) and present a nominal decomposition temperature of 200°C and 350 °C, respectively. AF particles have a density of 2.40 g/cm<sup>3</sup> and a BET surface area of 9 m<sup>2</sup>/g, while HF particles are characterized by a density of 2.36 g/cm<sup>3</sup> and a BET surface area of 9 m<sup>2</sup>/g. The selected fumed nanosilica was Aerosil<sup>®</sup> r974 (Ar974), surface treated with dimethyldichlorosilane and supplied by Evonik GmbH (Essen, Germany). Ar974 is characterized by a surface area of 170 m<sup>2</sup>/g, a bulk density of 1.99 g/cm<sup>3</sup> and a tap density of 60 g/l. This nanofiller is constituted by aggregates of equiaxed primary nanoparticles having an average size of 12 nm (SiO<sub>2</sub> content 99.8%). All the materials were used as received, without further purification.

### 2.2 Sample preparation

Polyethylene micro/nano-composite samples were produced through melt compounding in a Thermo Haake Poly-lab Rheomix internal mixer. Polymer granules and fillers

Table 1: List of the prepared samples

Sample name	PE (wt%)	AF (wt%)	HF (wt%)	Ar974 (wt%)
PE	100	-	-	-
PE-AF-10	90	10	-	-
PE-AF-20	80	20	-	-
PE-AF-30	70	30	-	-
PE-AF-40	60	40	-	-
PE-HF-10	90	-	10	-
PE-HF-20	80	-	20	-
PE-HF-25	75	-	25	-
PE-HF-30	70	-	30	-
PE-HF-40	60	-	40	-
PE-Ar974-2	97.9	-	-	2.1
PE-Ar974-4	95.8	-	-	4.2
PE-Ar974-10	90	-	-	10
PE-Ar974-20	80	-	-	20
PE-HF-20-Ar974-2	77.5	-	20	2.5
PE-HF-20-Ar974-5	75.2	-	20	4.8
PE-HF-20-Ar974-10	70	-	20	10
PE-HF-20-Ar974-20	60	-	20	20
PE-HF-30-Ar974-3	67.4	-	30	2.6
PE-HF-30-Ar974-5	64.8	-	30	5.2
PE-HF-30-Ar974-10	60	-	30	10
PE-HF-30-Ar974-20	50	-	30	20

were processed at 190°C for 10 minutes at 90 rpm. To avoid agglomeration, the fillers were added only after the complete melting of LLDPE. The resulting composites were subsequently hot-pressed in a Carver laboratory press at 170°C for 10 minutes, under a pressure of 2.5 MPa, to obtain square sheets of 200 × 200 × 1.5 mm<sup>3</sup>. A wide range of compositions were prepared, to investigate the effect of each of the two metal hydroxides and the fumed nanosilica separately, and then their synergistic influence on mechanical, thermal and fire performance. The samples will be identified as PE-AF/HF-*x*-Ar974-*y*, where “PE” stands for the polymer matrix, “AF” and “HF” indicate the aluminum and magnesium hydroxide particles, respectively, *x* indicates the weight fraction of the selected metal hydroxide with respect to the total mass of the sample, Ar974 stands for the fumed nanosilica and *y* represents its total weight fraction. In this study, *x* was varied in the range 10-40 wt% and *y* in the range 2-20 wt%. The compositions of all the prepared samples are reported in Table 1.

### 2.3 Experimental techniques

The size distributions of the two metal hydroxide FRs were measured with the laser granulometer LS13320 (Beckman Coulter) in the universal liquid module (ULM) with deionized water, at 900 rpm. The powders were put in suspension in deionized water before being introduced in the granulometer. The refractive index used was 1.589 for real part and 0.01 for the imaginary part.

The melt flow index (MFI) of the different compositions was measured with a Kayeness Co. 4003DE capillary rheometer, operating at 190°C with an applied load of 2.16 kg, according to the standard ASTM 1238.

The morphology of the composites and the distribution of the fillers were investigated through scanning electron microscopy (SEM), with a field-emission SEM Carl Zeiss AG SUPRA 40. The blends were cryofractured in liquid nitrogen and sputter-coated with a Pt-Pd alloy, in a Quorum Q150T sputtering machine.

Thermogravimetric analysis (TGA) was performed with a TA Q5000IR instrument, at a heating rate of 10 °C/min from room temperature to 700 °C. Specimens of approximately 10 mg were die-cut from the prepared sheets and tested in an air atmosphere with an air flux of

15 ml/min. From these tests, it was possible to evaluate the temperatures corresponding to a mass loss of 2%, 5% and 50% ( $T_{2\%}$ ,  $T_{5\%}$ ,  $T_{50\%}$ ), while the temperature of the maximum degradation rate ( $T_d$ ) was identified as the maximum of the mass loss derivative as a function of temperature.

Differential scanning calorimetry (DSC) was performed on the neat LLDPE matrix and on the composites with a Mettler DSC 30 calorimeter, to investigate the LLDPE crystallinity. Specimens of approximately 10 mg were die-cut from the prepared sheets and tested in the temperature range 0–200°C, with a heating/cooling rate of 10°C/min, under a nitrogen flux of 100 ml/min. The test consisted in a first heating scan, a cooling scan and a second heating scan. The LLDPE crystallinity ( $X_c$ ) was calculated with the expression reported in equation (1) as:

$$X_c = \frac{\Delta H}{\Delta H_0 \cdot W(PE)} \quad (1)$$

where  $\Delta H$  is the specific melting enthalpy of the samples (J/g),  $\Delta H_0$  is the theoretical heat of fusion of the 100% crystalline PE, equal to 293 J/g, and  $W(PE)$  is the LLDPE weight fraction. The Mettler DSC 30 instrument was also employed to carry out oxidation onset temperature (OOT) tests. These tests aimed to measure the temperature at which the material starts to degrade, under a constant heating rate. Specimens of approximately 10 mg were die-cut from the prepared sheets. The tests were performed following the ASTM E 2009 standard, under an air flux of 100 ml/min and a heating rate of 10°C/min from room temperature to 300°C, and the OOT was determined with the tangent method between the baseline and the degradation peak. The dehydration process of the as received metal hydroxides was studied with a Mettler DSC 20 in ambient atmosphere, from room temperature to 600°C, at a heating rate of 10°C/min.

Limiting oxygen index (LOI) tests were performed to measure the minimum oxygen concentration that sustains the combustion process. The material is said to burn with a given  $O_2$  concentration if the flame is able to top-down burn the specimen for a length of at least 50 mm in 3 minutes. According to the standard ASTM D 2683, rectangular specimens of  $100 \times 10 \times 4$  mm<sup>3</sup> were placed vertically inside a CEAST Oxygen Index apparatus. A blowtorch igniter was used to start the combustion process at the specimen's upper end. The flame propagation rate in air (at an  $O_2$  concentration of 20.8%) was also evaluated by measuring the time needed to burn 50 mm of the specimen.

Cone calorimetry is generally considered as the analysis that provides an all-round characterization of the flame behavior of a material. The technique is based on the measurement of the decreasing oxygen concentration in the

combustion gases of a sample subjected to a constant heat flux, which is then used to calculate the heat released per unit time and surface area, the heat release rate (HRR), measured in kW/m<sup>2</sup> [6]. Cone calorimetry tests were performed with a Fire Testing Technology cone calorimeter following the standard ISO 5660-1. Square specimens of  $100 \times 100 \times 3$  mm<sup>3</sup> were prepared via melt compounding and hot pressing and tested under a heat flux of 35 kW/m<sup>2</sup>, because this is a value close to that of the first stage of fire development. Besides the HRR value, it was also possible to determine the peak of the HRR (pHRR), the time-to-ignition (TTI) and the total heat released (THR). Furthermore, the test allowed the calculation of other parameters, such as (a) the fire performance index (FPI) as the ratio between TTI and pHRR, (b) the fire growth rate (FIGRA), as the maximum in HRR(time)/time, and (c) the maximum of average heat release emission (mAHRE) as a function of time.

Vicat tests were performed to determine the Vicat softening temperature (VST), defined as the temperature at which a flat-ended needle with a circular cross section of 1 mm<sup>2</sup> penetrates the specimen to a depth of 1 mm under a specific load and heating rate. According to the ASTM D 1525 standard, specimens with a surface area of approximately 1 cm<sup>2</sup> and a thickness of 3 mm were tested at a heating rate of 120°C/h and an applied load of 10 N.

The mechanical properties of the composites were investigated through uniaxial tensile tests, with an Instron 5969 universal testing machine equipped with a 50 kN load cell. Dumbbell 1BA specimens (standard UNI EN ISO 527-2) were die-cut from the prepared sheets. For the measurement of the elastic modulus, five specimens were tested for each composition at 0.25 mm/min, with a resistance extensometer Instron 2620-601 having a gauge length of 12.5 mm. The tests were stopped at a strain of 1% and the elastic modulus was evaluated with the secant method between the strain levels 0.05% and 0.25%. Tensile properties at break were performed at a crosshead speed of 100 mm/min on 1BA specimens. The resulting stress-strain curves were employed to obtain the values of stress at yield ( $\sigma_y$ ), stress at break ( $\sigma_b$ ) and strain at break ( $\epsilon_b$ ), while the tensile energy at break (TEB) was evaluated as the area under the stress-strain curve.

### 3 Results and discussion

Figure 1 reports the results of the granulometry test on the metal hydroxide FRs. The values of  $d_{10}$ ,  $d_{50}$  and  $d_{90}$  are 2.132, 4.988 and 11.24  $\mu\text{m}$  for AF and 1.753, 4.787 and

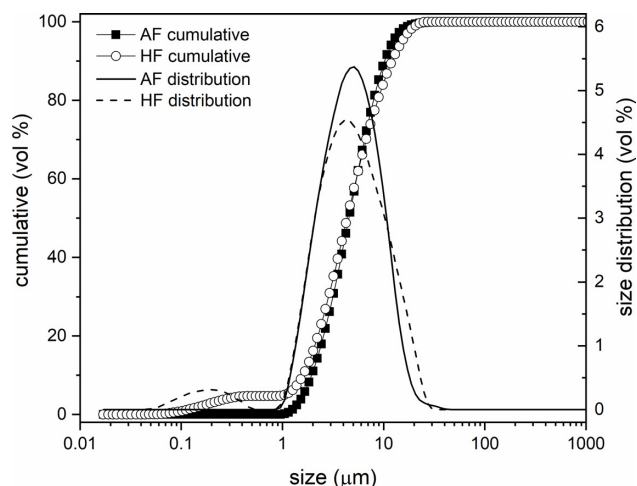
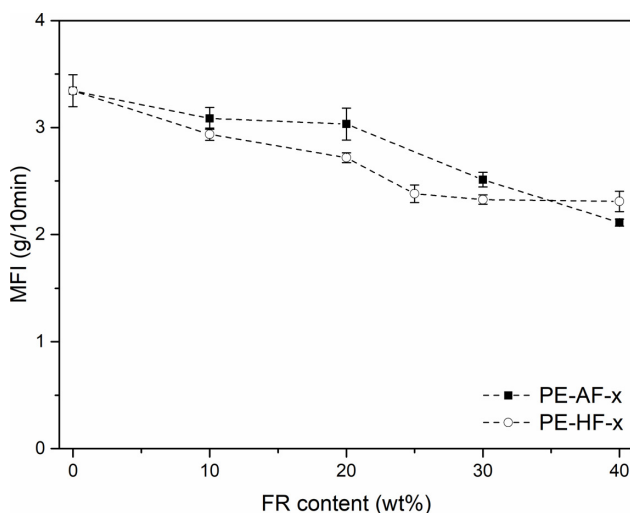


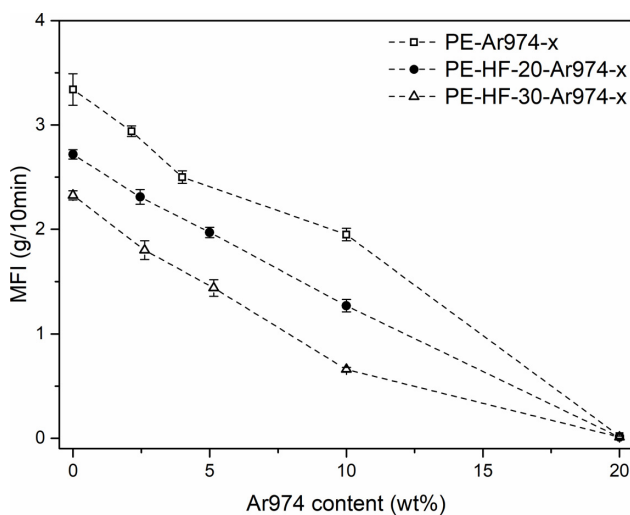
**Figure 1:** Results of the granulometry test on the metal hydroxide FRs. Particle size distribution and cumulative particle size distribution

13.33  $\mu\text{m}$  for HF. These results are in good agreement with the granulometry data reported on the technical data sheet provided by the producer.

Figure 2(a) reports the results of the MFI tests for the samples PE-AF-x and PE-HF-x ( $x = 0 \div 40$ ) compared with neat polyethylene (PE). In both cases, the MFI slightly decreases as the metal hydroxide content increases. The MFI values of these compositions range from  $3.34 \pm 0.15$  g/10 min, measured for the neat PE, to  $2.11 \pm 0.03$  g/10 min, determined for the sample PE-AF-40. This value, which is still 63 % of the MFI of the neat PE, indicates that the viscosity and the processability are not dramatically affected by the metal hydroxide content. On the other hand, the addition of fumed silica nanoparticles heavily decreases the MFI, as shown in Figure 2b. For the sample PE-Ar974-20, the measured MFI is  $0.02 \pm 0.01$  g/10 min, only 0.6% of the neat PE value. This effect is also evident in the formulations containing both metal hydroxides and nanosilica (Figure 2b). This dramatic impact of nanofillers on viscosity was expected, as it is reported elsewhere in the literature for different polymer-fumed nanosilica systems. This phenomenon is generally ascribed to the formation of a percolative network constituted by silica aggregates [3, 42–48], in good agreement with SEM results (see Figure 3d). The MFI test is one of the simplest techniques that give information on the melt fluidity. This parameter is important in this work not only because it relates to the processability of the material in the perspective to produce single-polymer composites, but also because the melt viscosity could influence the fire performance, especially the heat-release rate measured in cone calorimetry tests, as reported by several studies [33, 49–51].



(a)



(b)

**Figure 2:** (a) MFI values of the samples PE, PE-AF-x and PE-HF-x ( $x = 10 \div 40$ ) as a function of the FR weight fraction; (b) MFI values of the samples PE-Ar974-x, PE-HF-20-Ar974-x and PE-HF-30-Ar974-x ( $x = 2 \div 20$ )

A higher melt viscosity has often been correlated with an improved flame resistance, as a highly viscous polymer bulk promotes the formation of a compact charred layer and avoids the sinking of the additives in the polymer melt layer, which is also favored by additives with low density and high surface area [6], such as the fumed nanosilica. On the other hand, low viscosity promotes the early cracking of the charred layer [33] and favors the growth of bubbles and their migration towards the burning surface, which increases the supply of the flame with the pyrolysis gases [49]. Therefore, the aimed viscosity in this work should be an intermediate value, as a higher viscosity could be beneficial for the flame resistance of the ma-

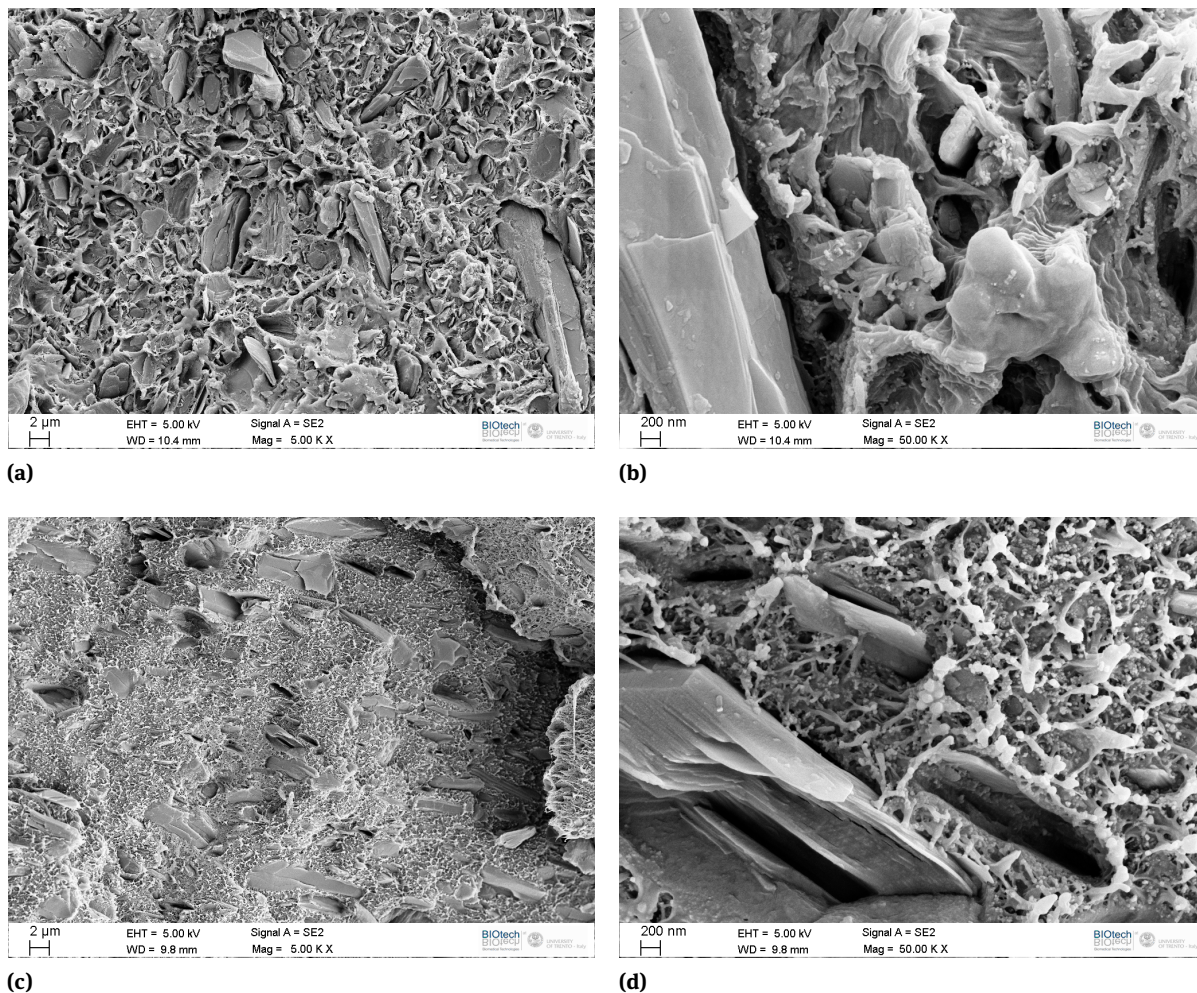


**Figure 3:** SEM micrographs of the cryofracture surface of the prepared samples: (a) PE-HF-30-Ar974-3, 5 kX; (b) PE-HF-30-Ar974-3, 70 kX; (c) PE-HF-30-Ar974-20, 5 kX; (d) PE-HF-30-Ar974-20, 70 kX.

terial, but the processability is also an important aspect to be preserved.

Figure 3(a-d) report SEM micrographs at different magnifications of the cryofracture surface of some selected compositions containing both HF and nanosilica. These micrographs highlight the morphology and dispersion of the micro- and nano-fillers. SEM micrography was performed also on AF-containing samples, but the micrographs are not reported for the sake of brevity, as the fracture surface, the adhesion properties and the morphology of the metal hydroxide particles are very similar to those of the samples containing HF. The HF is in the form of micrometric particles with a non-equiaxed, lamellar structure and a rough surface. The particles are well dispersed in the PE matrix, do not form agglomerates, and seem to be weakly bonded to the polymer matrix. The nanosilica, as it results from Figure 3(c-d), is present in the form of aggre-

gates with dimensions of tens of nanometers, which are well dispersed in the polymer matrix. The percolative network formed by silica nanoparticles is visible in these SEM micrographs, and it is also the reason of the improvement of the mechanical properties such as the elastic modulus and the stress at break [40, 52, 53].

DSC tests were carried out to measure the degradation temperature of the metal hydroxides and the effect of filler addition on the crystallinity of LLDPE ( $X_c$ ). The measured degradation (dehydration) temperatures are 319°C for AF and 422°C for HF. The temperature degradation interval of HF is closer to that of LLDPE, as observed in TGA tests. The investigation of the influence of the fillers on the LLDPE crystallinity was limited to the samples containing only the metal hydroxides, *e.g.* PE-AF-x and PE-HF-x, as their effect on the crystallization behavior of a polyethylene matrix has been less investigated than that of fumed nanosil-

ica, which has already been studied by this group [43, 47]. The obtained results are summarized in Table 2.

It can be observed that the melting and crystallization temperatures are not substantially affected by the introduction of the metal hydroxides, while the crystallinity content increases from 39.0% for the neat PE to 42.2% for a metal hydroxide content of 40 wt%. Moreover, the crystallization temperature increases with an increase in the metal hydroxide content. This suggests that both AF and HF particles may act as nucleating agents, thereby favoring the nucleation and growth of crystals within the polymer matrix.

The TGA analysis performed in air allowed the investigation of the resistance to the thermo-oxidative degradation of the prepared materials. Representative TGA thermograms of some selected compositions are reported in Figure 4. The temperatures corresponding to a mass loss of 2%, 5% and 50% ( $T_{2\%}$ ,  $T_{5\%}$ ,  $T_{50\%}$ ), and the temperature associated to the maximum degradation rate ( $T_d$ , see Paragraph 2.3) are summarized in Table 3.

TGA tests in air were also performed on the flame retardants as received, and the measured  $T_d$  for AF and HF were 276°C and 382°C, respectively, which are in good agreement with the decomposition temperatures declared by the producer. All the temperatures reported in Table 3 for HF are close to those measured for the neat PE, while AF decomposes at lower temperatures. This lead to the lowering of  $T_{2\%}$  of the samples PE-AF-x as the AF content increases. On the other hand, all the degradation temperatures generally increase with the HF content. This is an indication that the HF is more efficient in subtracting heat when required, thus being probably the most suitable flame retardant for PE, even though the coincidence of the decomposition intervals of the FR and polymer matrix is not the only criterion to be considered, since, as mentioned before, the heat subtraction through the endothermic reaction is not the only fire retardant mechanism of mineral fillers [13]. An improvement of the thermo-oxidative degradation behavior is also observed for the samples containing nanosilica, but only at low concentrations. This is evident both when the nanosilica is present alone (samples PE-Ar974-x) and when it is combined with HF (samples PE-HF-20-Ar974-x and PE-HF-30-Ar974-x). The increased thermal stability of polymer matrices due to the addition of nanofillers is generally ascribed to the fact that the nanofiller accumulates and agglomerates on the surface of the degrading polymer, thereby creating a protective barrier that delays the volatilization of the low molecular weight degradation products [40, 54]. The decrease in  $T_{2\%}$  and  $T_{5\%}$  at high silica content was previously observed in the literature and it can be explained with the

degradation of thermally labile organic species introduced with the surface modification of nanosilica [40, 55, 56]. It is interesting to note that the substitution of the 5 wt% of HF with nanosilica improves the thermo-oxidative resistance, as the values of  $T_{2\%}$ ,  $T_{5\%}$ ,  $T_{50\%}$  and  $T_d$  for the sample PE-HF-20-Ar974-5 are higher than those of the sample PE-HF-25. This suggests that the two fillers act synergistically to enhance the thermal stability of the matrix.

The same trends observed in TGA were also recorded in OOT tests. Some representative OOT curves are reported in Figure 5, while Figure 6(a-b) summarizes the OOT values as a function of the weight fraction of the metal hydroxides and the nanosilica.

Both metal hydroxides lead to an increase in the OOT of approximately 20°C with a filler content of 40 wt%. However, the increase in OOT is not linearly related to the filler content, but it reaches a plateau value of 232-235°C. The same increase in OOT was also observed after the introduction of nanosilica, and the specimens containing both the nanosilica and one of the two metal hydroxides present an OOT value higher than those containing only one filler type. It is interesting to note that the sample PE-HF-25 manifests an OOT of 232.7°C, while an OOT of 238.2°C was measured for the sample PE-HF-20-Ar974-5, which has the same total filler content (25 wt.%) but combines both filler types. This highlights once again the synergistic effect of the employed micro- and nanofillers in enhancing the thermal stability of LLDPE.

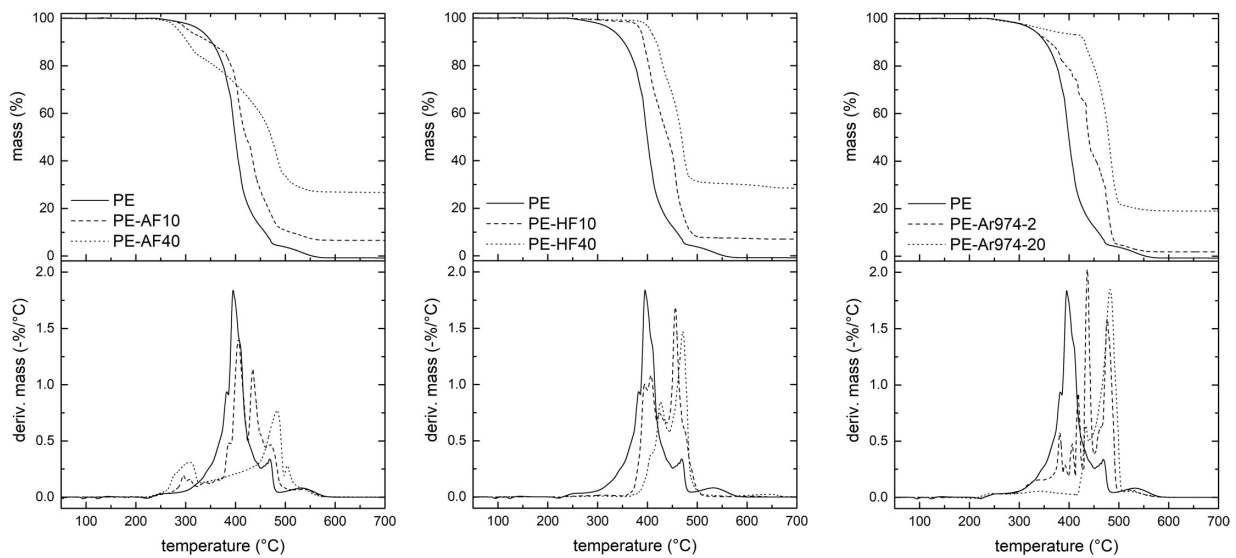
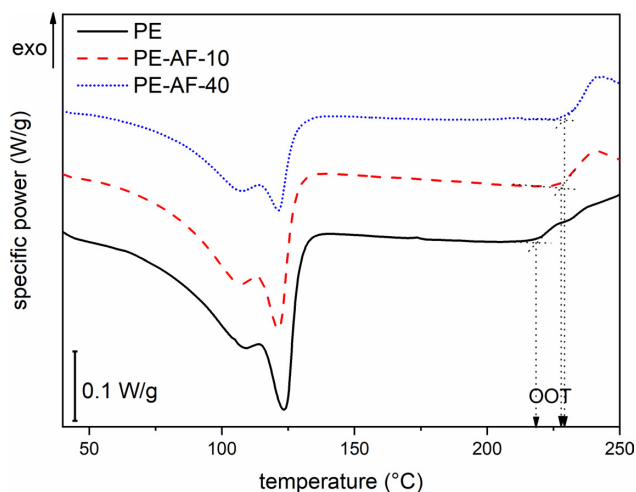
The introduction of non-halogenated products able to improve flame retardancy and simultaneously preserve or even improve the mechanical performance of the polymer matrices could be very attractive from an applicative point of view, and both nanosilica and metal hydroxides are good candidates in this sense. The mechanical properties of these compositions were investigated through uniaxial tensile test, and Figure 7 shows representative stress-strain curves. First, the effect of the two metal hydroxides on the mechanical properties of LLDPE was investigated, and the most important results are summarized in Table 4.

Both AF and HF considerably increase the elastic modulus of LLDPE. The stiffness of the material increases with the filler content. A maximum value of 566 MPa, *i.e.* 300% higher than the modulus of unfilled LLDPE, is reached for an HF loading of 40 wt%. These results are in good agreement with those reported in the literature for similar systems [14, 24], and it was an expected result that reasonably follows the addition of a stiffer filler. The same trend is observable on the stress at yield ( $\sigma_y$ ), even though to a lower extent. On the other hand, the addition of metal hydroxides causes a decrease in the strain at break ( $\epsilon_b$ ), and thus of the stress at break ( $\sigma_b$ ) due to the reduction of the strain

**Table 2:** Main results of the first DSC heating scan for some selected compositions

Sample	$T_m$ (°C)	$\Delta H_m$ (J/g)	$X_c$ (%)	$T_c$ (°C)	$\Delta H_c$ (J/g)
PE	121.2	113.0	39.0	104.0	107.1
PE-AF-10	121.1	110.2	42.2	105.3	102.2
PE-AF-40	120.9	73.5	42.2	109.0	64.6
PE-HF-10	121.2	106.3	40.7	105.2	99.3
PE-HF-40	121.0	73.3	42.2	107.3	67.1

$T_m$ ,  $T_c$  = melting and crystallization temperatures;  $\Delta H_m$ ,  $\Delta H_c$  = melting and crystallization enthalpies;  $X_c$  = crystallinity

**Figure 4:** Representative TGA thermograms in air of PE and PE-AF- $x$  ( $x = 10, 40$ ), PE-HF- $x$  ( $x = 10, 40$ ), and PE-Ar974- $x$  ( $x = 2, 20$ )**Figure 5:** Representative OOT thermograms of the samples PE-AF- $x$  ( $x = 10, 40$ )

hardening region. In any case, a metal hydroxide content of 20 wt.% causes a reduction of about 24% in strain at break with respect to the unfilled matrix, and corresponds to a value of  $\epsilon_b$  still above 1000%, while a metal hydrox-

ide content of 40 wt.% deteriorates dramatically the plastic resources of the matrix, as the failure happens immediately after the yield point. The failure properties are comparable to those reported for similar systems in the literature [18]. The decrease in ductility is one of the reasons why the metal hydroxide content of the samples containing also the fumed nanosilica was limited at 30 wt.%. This content can be considered a good compromise between melt fluidity, stiffness, ductility and thermal stability.

Figure 8(a-c) reports the mechanical properties of the samples containing fumed nanosilica alone and in combination with 20 and 30 wt% of HF, e.g. the samples PE-Ar974- $x$ , PE-AF-20-Ar974- $x$  and PE-AF-30-Ar974- $x$  ( $x = 0 \div 20$ ). In these figures the values of  $E$ ,  $\sigma_y$  and  $\epsilon_b$  of the composites as a function of the nanosilica weight fraction have been normalized to those of the blends with the same metal hydroxide content but without nanosilica, e.g. PE, PE-HF-20 and PE-HF-30. In this way, the contribution of nanosilica on the mechanical properties can be highlighted. The presence of nanosilica gives a positive contribution to the elastic modulus (Figure 8a) and stress at yield (Figure 8b) for all the nanosilica contents. Moreover, it also

Table 3: Results of the TGA tests in air

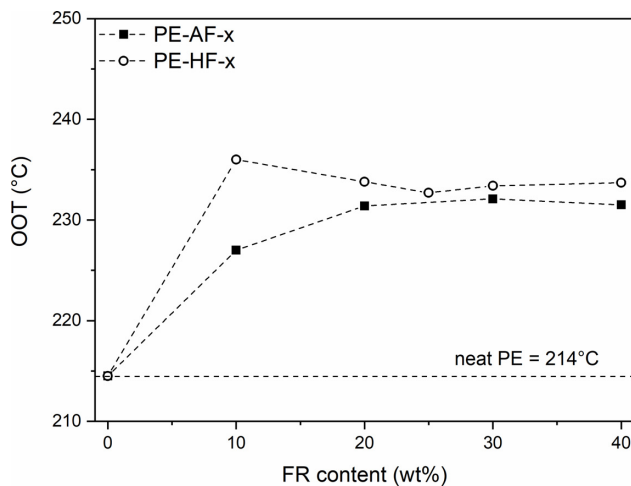
Sample	T <sub>2%</sub>	T <sub>5%</sub>	T <sub>50%</sub>	T <sub>d</sub> (°C)	m <sub>r</sub> (%)
PE	295.6	329.2	400.0	395.3	0.00
AF	215.3	240.7	-	276.3	65.40
HF	315.5	349.0	-	382.3	69.03
PE-AF-10	286.4	306.0	421.4	406.2	6.62
PE-AF-20	279.6	297.0	446.9	424.3	13.47
PE-AF-30	274.0	292.0	443.7	442.4	19.90
PE-AF-40	270.3	285.4	471.8	483.7	26.71
PE-HF-10	371.6	385.8	440.6	456.1	7.08
PE-HF-20	380.3	393.2	450.6	458.8	14.28
PE-HF-25	377.1	392.1	458.7	469.0	17.20
PE-HF-30	394.2	404.7	453.8	457.6	21.46
PE-HF-40	392.3	405.6	468.7	471.1	28.50
PE-Ar974-2	298.5	329.3	439.3	437.0	1.83
PE-Ar974-4	285.6	330.5	464.6	489.0	4.03
PE-Ar974-10	276.3	334.3	479.1	490.5	10.03
PE-Ar974-20	296.0	359.7	479.4	482.4	19.04
PE-HF-20-Ar974-2	359.9	383.4	471.0	480.5	16.87
PE-HF-20-Ar974-5	359.9	401.0	479.9	483.3	18.15
PE-HF-20-Ar974-10	348.7	396.3	475.9	476.9	23.87
PE-HF-20-Ar974-20	336.8	381.3	453.6	439.9	33.12
PE-HF-30-Ar974-3	387.4	403.9	460.8	466.4	22.83
PE-HF-30-Ar974-5	380.2	405.0	475.2	479.8	24.86
PE-HF-30-Ar974-10	373.1	398.9	464.8	465.8	30.95
PE-HF-30-Ar974-20	306.7	336.4	460.7	450.9	40.21

Table 4: Results of the tensile test on the samples PE-AF-x and PE-HF-x (x = 10 ÷ 40)

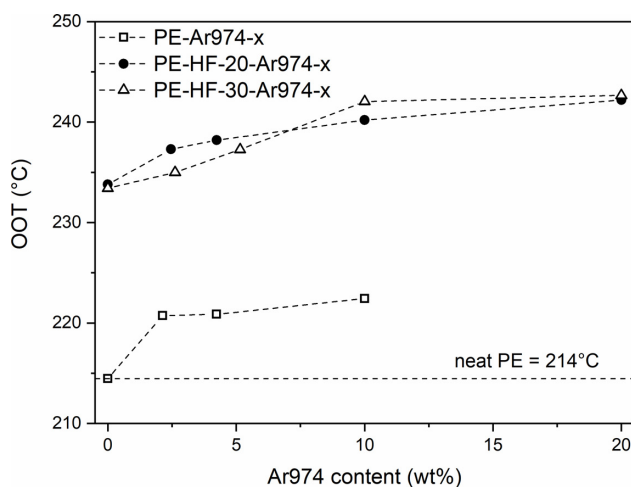
Sample	E (MPa)	$\sigma_y$ (MPa)	$\sigma_b$ (MPa)	$\epsilon_b$ (%)	TEB (mj/mm <sup>3</sup> )
PE	189 ± 38	9.8 ± 0.2	17.4 ± 2.1	1446 ± 198	172 ± 33
PE-AF-10	299 ± 41	10.3 ± 0.1	15.2 ± 3.0	1214 ± 236	133 ± 38
PE-AF-20	377 ± 32	10.7 ± 0.1	13.3 ± 1.0	1064 ± 61	106 ± 9
PE-AF-30	443 ± 19	11.2 ± 0.1	8.4 ± 2.1	526 ± 306	45 ± 25
PE-AF-40	566 ± 14	11.6 ± 0.1	7.3 ± 3.2	79 ± 56	7 ± 4
PE-HF-10	198 ± 17	10.9 ± 1.3	18.3 ± 2.1	1356 ± 36	166 ± 16
PE-HF-20	290 ± 39	10.4 ± 0.2	13.4 ± 0.5	1098 ± 62	110 ± 10
PE-HF-25	321 ± 43	10.5 ± 0.3	9.8 ± 0.7	815 ± 44	81 ± 3
PE-HF-30	344 ± 70	10.8 ± 0.1	6.6 ± 2.8	460 ± 339	39 ± 30
PE-HF-40	507 ± 48	11.0 ± 0.1	4.3 ± 0.9	92 ± 64	8 ± 5

increases the strain at break of the blends (Figure 8c), but only at low weight fractions. In a recent work of our group a new theoretical model was proposed to demonstrate that nanofiller aggregation may constrain a portion of matrix, thus limiting the mobility of macromolecules [57]. The stiffening effect of fumed nanosilica is well documented in the literature [3], as well as the effect on the stress at yield and the strain at break [58]. These results highlight that

the sample PE-AF-20-Ar974-5 has a good compromise between stiffness, strength and ductility, and therefore it is the best candidate in the perspective of fabricating single-polymer composites, from the mechanical point of view. It is interesting to notice that the synergistic effect between metal hydroxides and nanosilica is visible also on the mechanical properties, as the sample PE-HF-20-Ar974-5 had



(a)



(b)

**Figure 6:** OOT values of (a) PE-AF-x and PE-HF-x ( $x = 10 \div 40$ ) samples as a function of the FR weight fraction; (b) PE-Ar974-x, PE-HF-20-Ar974-x and PE-HF-30-Ar974-x ( $x = 0 \div 20$ ) samples as a function of the Ar974 weight fraction

higher elastic modulus, yield strength and also elongation at break than the sample PE-HF-25.

Table 5 summarizes the results of the Vicat tests on the samples PE, PE-HF20-Ar974-x and PE-HF30-Ar974-x ( $x = 0 \div 20$ ). The measured Vicat softening temperature (VST) of the neat PE is  $100.8 \pm 1.4^\circ\text{C}$ , i.e. slightly higher than the value of  $96^\circ\text{C}$  declared by the producer. For low filler concentrations, the VST is not significantly different from that of neat PE, while it increases with an increase in silica content at elevated concentrations, up to  $113.0^\circ\text{C}$  for the PE-HF30-Ar974-20 sample, which corresponds to an increase of  $12^\circ\text{C}$  with respect to the unfilled polymer.

On the basis of the results presented so far, a selection of optimal compositions can be made according to the me-

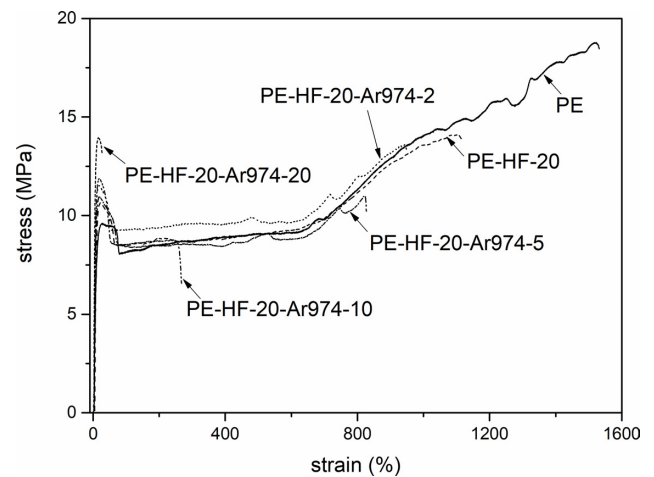


**Figure 7:** Representative tensile stress-strain curves of PE, PE-HF-20 and PE-HF-20-Ar974-x ( $x = 2 \div 20$ )

**Table 5:** Vicat softening temperature (VST) of the prepared samples

Sample	VST ( $^\circ\text{C}$ )
PE	$100.8 \pm 1.4$
PE-HF-20	$99.7 \pm 2.0$
PE-HF-20-Ar974-2	$100.0 \pm 0.6$
PE-HF-20-Ar974-5	$101.0 \pm 1.5$
PE-HF-20-Ar974-10	$101.8 \pm 1.2$
PE-HF-20-Ar974-20	$105.6 \pm 0.2$
PE-HF-30	$98.7 \pm 1.2$
PE-HF-30-Ar974-3	$100.7 \pm 1.9$
PE-HF-30-Ar974-5	$103.3 \pm 1.4$
PE-HF-30-Ar974-10	$105.9 \pm 2.8$
PE-HF-30-Ar974-20	$113.0 \pm 1.7$

**Table 6:** LOI and propagation rate in air of the prepared samples

Sample	LOI (%)	Propagation rate in air (mm/s)
PE	18.5	0.43
PE-HF-20	29.6	0.10
PE-HF-25	30.7	0.09
PE-Ar974-2	22.3	0.30
PE-Ar974-4	24.8	0.15
PE-HF-20-Ar974-2	31.9	n.d.*
PE-HF-20-Ar974-5	35.2	n.d.*

\*n.d. not detectable

chanical and thermal properties, but also on the processability and melt viscosity, in the perspective to use these materials as matrices for singlepolymer composites. The most promising metal hydroxide is HF, as it has a decomposition temperature closer to the degradation tempera-

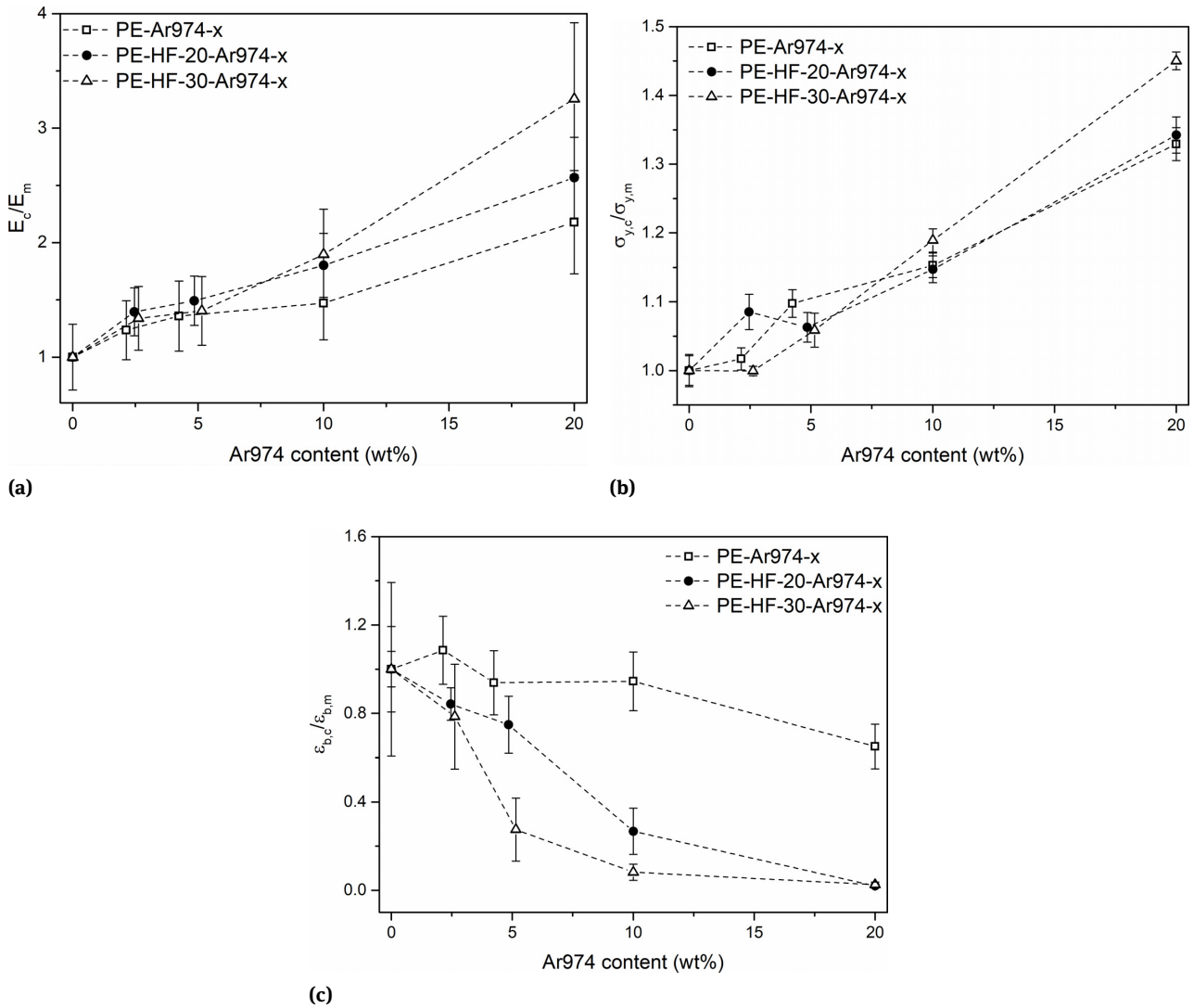


**Figure 8:** Relative tensile properties of the samples PE-Ar974-x, PE-HF-20-Ar974-x and PE-HF-30-Ar974-x (x = 0 ÷ 20), normalized to those of the samples PE, PE-HF-20 and PE-HF-30, respectively: (a) elastic modulus; (b) stress at yield; (c) strain at break

**Table 7:** Results of cone calorimetry tests on the prepared samples

Sample	TTI (s)	pHRR (kW/m <sup>2</sup> )	THR (MJ/m <sup>2</sup> )	FPI	FIGRA (kW/s·m <sup>2</sup> )	mAHRE (kW/m <sup>2</sup> )
PE	129	712	188	0.18	2.2	311
PE-HF-20	124	302	178	0.41	1.8	188
PE-HF-25	124	267	171	0.46	1.6	171
PE-Ar974-2	138	712	215	0.19	2.1	339
PE-Ar974-4	142	672	220	0.21	1.9	322
PE-HF-20-Ar974-2	110	274	188	0.40	1.8	177
PE-HF-20-Ar974-5	115	246	181	0.47	1.6	147

TTI = time-to-ignition, pHRR = peak of heat-release rate, THR = total heat released, FPI = fire performance index (FPI = TTI/pHRR), FIGRA = fire growth rate, mAHRE = maximum of average heat release emission

ture of LLDPE, thus being more suitable to subtract heat when needed. In order to preserve the ductility of the polymer matrix, the content of HF should be limited to 20-30 wt%. To retain the melt fluidity and have an acceptable MFI value to preserve the processability, the nanosilica content was limited to a maximum of 5 wt%. Two tests were performed to investigate the flame resistance of the samples with optimized composition, namely the limiting oxygen index (LOI) and the cone calorimetry tests.

The results of the LOI test are reported in Table 6, which summarizes the values of LOI (%) and the flame propagation rate in air (mm/min). The measured LOI for LLDPE was 18.5%, which is in good agreement with values commonly reported in the literature for polyethylene [2] and classifies this polymer as inflammable and self-sustaining the combustion [1]. The LOI increases with an increase in the HF weight fraction, reaching 30.7% with an HF content of 25 wt.%, and also with an increase in the nanosilica loading, up to 24.8% for a nanosilica content of 4 wt.%. The opposite trend is observed for the flame propagation rate in air, which strongly decreases with an increase in the filler content. The highest LOI values were measured on the two samples containing both HF and nanosilica, with a maximum of 35.2% for the sample PE-HF-20-Ar974-5. For these two samples, it was not possible to measure the flame propagation rate in air, as these compositions are self-extinguishing and the flame was not able to burn the specimen for the 50 millimeters used as a reference to measure the propagation rate. For PE-HF-20-Ar974-2, the flame ceased to burn after 9 min and 36 s, while the flame on PE-HF-20-Ar974-5 took a shorter time to completely self-extinguish (45 s). In both cases, however, the flame was very small and it clearly had difficulties in top-down burning the sample. It is interesting to note that the sample PE-HF-25, containing the 25 wt% of HF, has a lower LOI than the sample PE-HF-20-Ar974-5, which contains the same total amount of fillers but combining HF and nanosilica. This increase in the LOI value from 30.7% to 35.2% is an additional evidence of the synergistic effect played by the combination of the two selected fire retardants. This positive combined effect could be the consequence of the increased viscosity imparted by the presence of nanosilica. It should be noted that the MFI value of PE-HF-20-Ar974-5 is  $1.97 \pm 0.05$  g/10 min, and it is lower than the MFI values of both PE-HF-20 ( $2.72 \pm 0.05$ ) and PE-HF-25 ( $2.38 \pm 0.08$  g/10 min). This implies a higher melt viscosity, which helps preventing dripping and promoting char formation.

It is also interesting to observe the different burning mechanisms of the samples containing the investigated fire retardants. Figure 9(a-d) reports representative images of the burning samples during the LOI analysis. The sam-

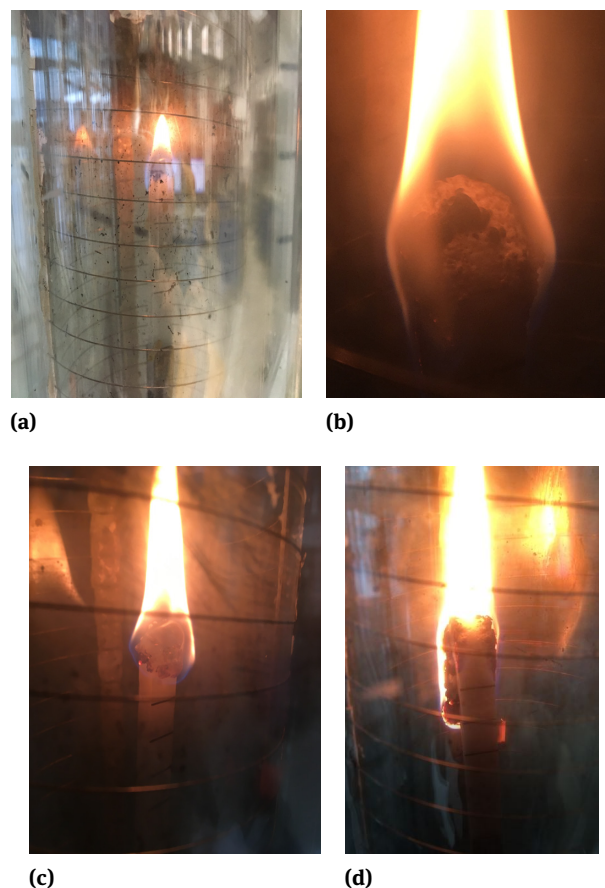


**Figure 9:** Representative images of the LOI analysis of the samples: (a) PE at 21.0 O<sub>2</sub>%; (b) PE-HF-25 at 28.3 O<sub>2</sub>%; (c) PE-Ar974-2 at 25.7 O<sub>2</sub>%; (d) PE-HF-20-Ar974-5 at 33.1 O<sub>2</sub>%

ples containing HF (Figure 9b) develop a sponge-like structure due to the water release at the burning surface, with the formation of bubbles, while the samples containing nanosilica (Figure 9c) form a char layer that prevents drips and hinders the diffusion of oxygen inside the material.

The samples containing both fillers develop a burning zone with both characteristics, even though the formation of bubbles is strongly reduced, which can be the consequence of the increased viscosity. The same structures can be observed also in Figure 10, showing the samples after the LOI test.

Cone calorimetry is regarded as the most complete medium-sized test to investigate the fire behavior of polymers. Curves of heat-release rate and total heat released for all the tested samples are reported in Figure 11(a-b), while the most important results are summarized in Table 7.

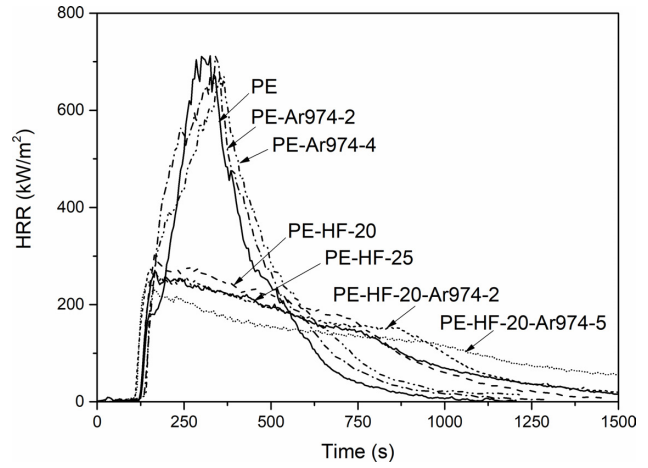
The addition of nanosilica at such low weight fractions (up to 4 wt%) slightly increases the TTI and decreases the pHRR, and the shape of the curves on Figure 11a are



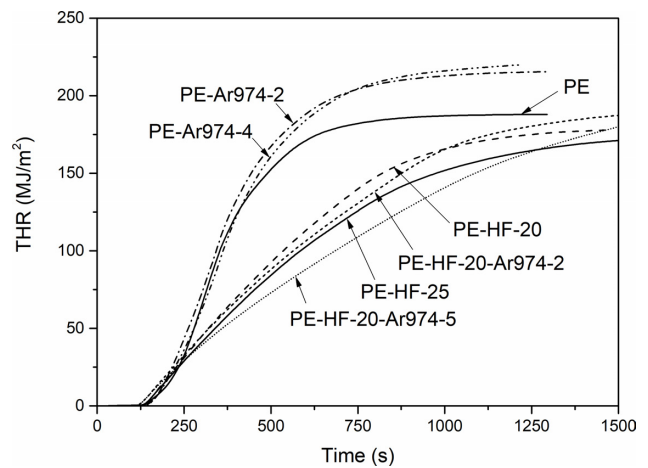
**Figure 10:** Samples after the LOI analysis. From left to right: PE, PE-HF-20, PE-HF-25, PE-Ar974-2, PE-Ar974-4, PE-HF-20-Ar974-2 and PE-HF-20-Ar974-5

substantially the same as those of the neat PE. On the other hand, the addition of metal hydroxides leads to a considerable reduction in the pHRR, which decreases from 712 kW/m<sup>2</sup> for the neat PE to 267 kW/m<sup>2</sup> for the PE-HF-25 sample, with a reduction of 63%. This reduction is also appreciable from the curve shapes in Figure 11a. In the same way, other important fire-related parameters are improved, such as the FPI, which increases from 0.18 to 0.46, and the mAHRE, which decreases from 311 kW/m<sup>2</sup> to 171 kW/m<sup>2</sup>. The same behavior is presented by the samples containing both HF and Ar974, which show a better fire performance than the neat PE. The photographs of the residues of the specimens after the tests are reported in Figure 12(a-f). It can be noticed that cohesive residues are formed with a silica content of 4 wt%, even without magnesium hydroxide. Moreover, the dark color of residues containing silica indicates that this nanofiller tends to promote charring.

These tests highlight the synergistic effect between the metal hydroxide microfiller and fumed silica nanofiller, since the sample PE-HF-20-Ar974-5 shows better fire performances than the sample PE-HF-25 in terms of pHRR, mAHRE and FPI values. Being the FPI the ratio between the TTI and the pHRR, a high FPI suggests that this composition has a quite long time to ignition and at the same time it does not rapidly burn releasing smoke. Once again, the synergistic effect and the positive contribution of the fumed silica could be partly ascribed to the increase in the melt viscosity. To highlight the correlation between the melt viscosity and the fire performance, Figure 13(a-b) report the values of pHRR, LOI and FIGRA, normalized to the values of the neat PE, as a function of the MFI and the melt volume index (MVI), calculated by dividing each value of MFI by the melt density. It can be observed that the fire performance increases with a decrease in MFI and



(a)



(b)

**Figure 11:** Cone calorimetry curves of the samples PE, PE-HF-*x* (*x* = 20, 25), PE-Ar974-*x* (*x* = 2, 4), PE-HF-20-Ar974-*x* (*x* = 2, 5): (a) HRR as a function of time; (b) THR as a function of time

MVI, with an almost linear trend for the values LOI and FIGRA as a function of the MVI. This result is in good agreement with similar results reported in the literature for correlations between pHRR and other rheological parameters such as the shear storage modulus  $G'$  [33, 49, 50], and suggests that important information on the fire behavior can be provided also by a simple rheological test such as the MFI. In this plot, the values corresponding to the samples PE-HF-25 and PE-HF-20-Ar974-5 are highlighted to underline the better flame performance of the sample combining the two fillers. This representation suggests that the rise in viscosity could contribute to the synergistic effect between metal hydroxides and nanosilica. Finally, Figure 14 summarizes all the results of the characterization and evidences that the sample PE-HF-20-Ar974-5 outperforms PE-HF-25 not only in several properties related to

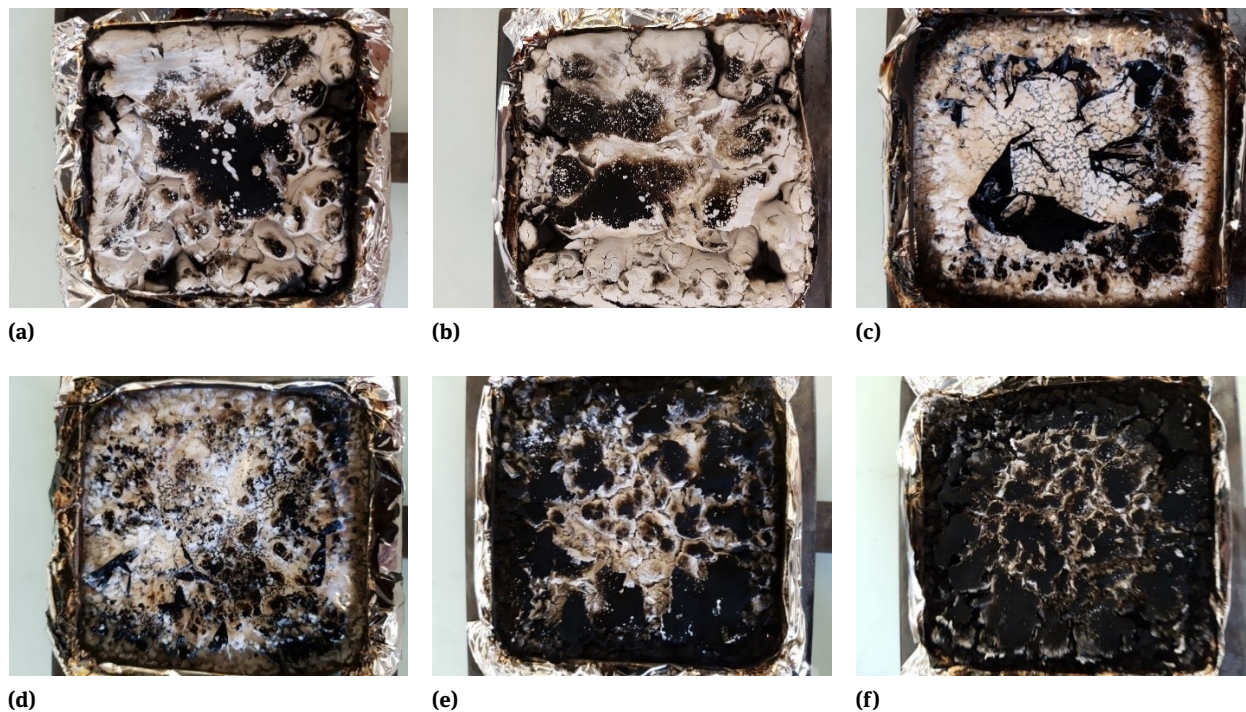


**Figure 12:** Images of the specimens after the cone calorimetry tests. (a) PE-HF-20; (b) PE-HF-25, (c) PE-Ar974-2; (d) PE-Ar974-4; (e) PE-HF-20-Ar974-2; (f) PE-HF-20-Ar974-5

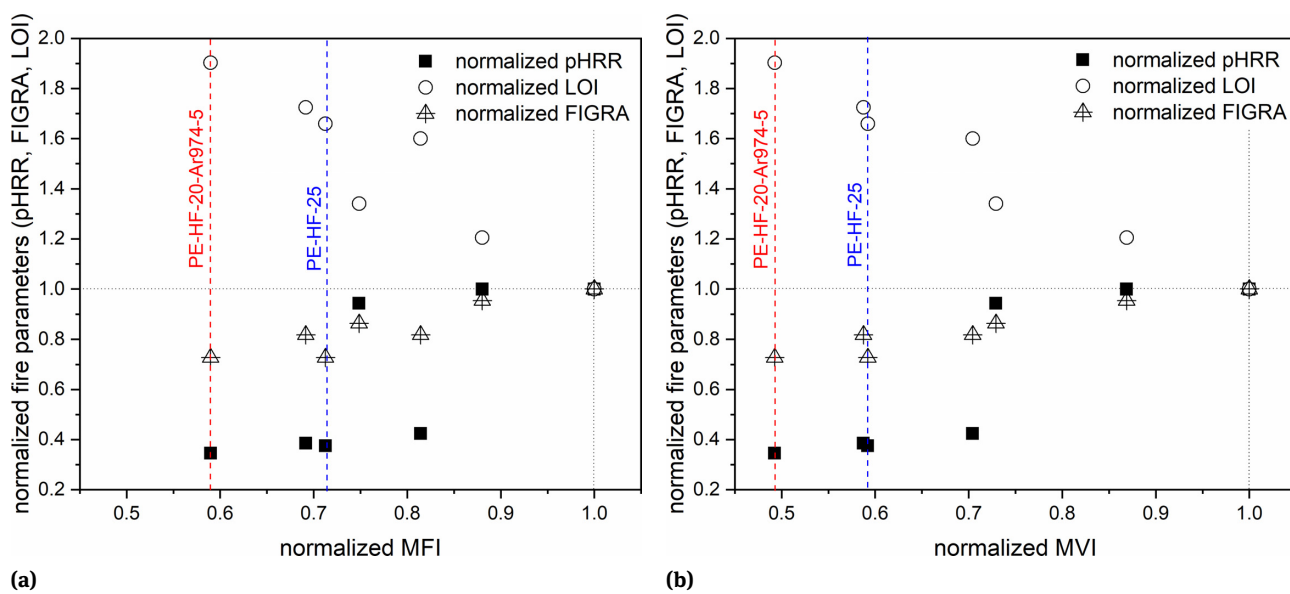


**Figure 13:** Normalized fire parameters (pHRR, FIGRA, LOI) versus normalized MFI (a) and MVI (b)

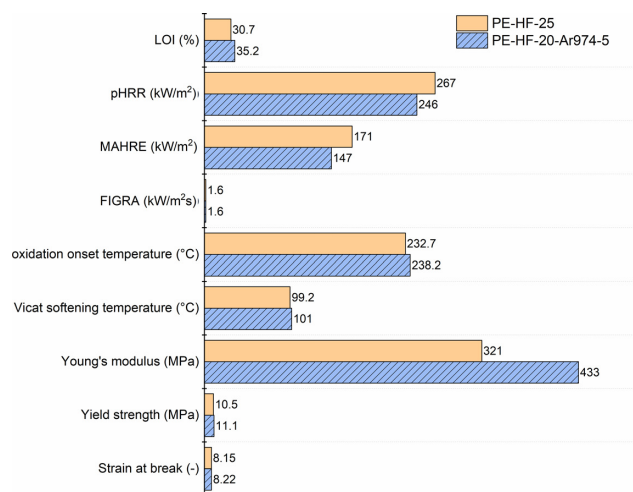


**Figure 14:** Results of the characterization on the samples PE-HF-25 and PE-HF-20-Ar974-5

fire retardancy and resistance to thermo-oxidative degradation, but also in some mechanical parameters, thereby highlighting the synergistic effect of the two fillers also in enhancing the mechanical properties of the microcomposite.

## 4 Conclusions

In this work, LLDPE-based micro/nanocomposites were prepared by using surface functionalized fumed silica nanoparticles and two kinds of metal hydroxides (aluminum trihydroxide and magnesium hydroxide) at different relative amounts. The work aimed at investigating the FR capability to improve the flame properties, the thermal degradation performance and the mechanical properties of the matrix, and to evaluate synergistic effects between micro- and nanofillers.

SEM images revealed that both metal hydroxide microparticles and fumed silica aggregates were homogeneously distributed within the matrix, and silica created a percolative network at elevated concentrations. The measurement of MFI showed that the melt fluidity and the processability of the composites was not seriously impaired upon AF and HF introduction, while nanosilica loadings higher than 5 wt.% led to an unacceptable reduction of the MFI values.

TGA and OOT tests demonstrated that HF was more efficient than AF in subtracting heat in the temperature interval required by LLDPE, while the nanosilica was responsible for an important improvement in the thermal degradation behavior. It was interesting to note that the thermal

degradation properties measured with TGA and OOT tests were better in the sample in which 5 wt.% of HF was substituted by nanosilica than in that containing only HF, at the same total filler concentration (25 wt.%), which suggests a synergistic effect between the two fillers.

Tensile tests on the prepared materials showed that both metal hydroxides promoted an important increase in elastic modulus and yield strength, and even though this was accompanied by a strong deterioration of the strain at break, the reduction in ductility was unacceptable only at high metal hydroxide concentrations. The introduction of small amounts of nanosilica helped to partially retain the failure properties of the pristine matrix. It was interesting to note that the synergistic effect between metal hydroxides and nanosilica is visible also on the mechanical properties, as the sample PE-HF-20-Ar974-5 had higher elastic modulus, yield strength and also elongation at break than the sample PE-HF-25.

Lastly, LOI and cone calorimetry tests on the samples with optimized compositions demonstrated that the synergistic effect between HF and fumed silica at a proper relative ratio could lead to a strong enhancement of the fire performance. An interesting correlation was found between normalized fire parameters (pHRR, FIGRA and LOI) and normalized viscosity parameters (MFI and MVI), which suggests that a simple test such as the MFI can be useful to provide information on the flame performance.

Unless similar works, this research activity has focused on the investigation not only of the effect of FRs on the fire performance and the resistance to thermo-oxidative degradation of the polymer matrix, but also of the corresponding mechanical, physical and processing-related properties. Moreover, this research has addressed the flame retardancy enhancement given by the combination of metal hydroxides and isodimensional fillers such as fumed silica nanoparticles, which are less widely used as a flame retardant synergist than other nanofillers, even though they have been proven effective in enhancing the mechanical properties and the fire performance of polymers.

Given all the presented results concerning the processability, the mechanical properties, the thermo-oxidation resistance and the fire performance, the sample PE-HF-20-Ar974-5 was evaluated as the most suitable composition to be employed to fabricate fire resistant PE-based single polymer composites with the introduction of UHMWPE fibers, as confirmed by preliminary encouraging results.

**Acknowledgement:** Mr. Andrea De Col is gratefully acknowledged for his support to the experimental work. Mr.

Loic Dumazert is gratefully acknowledged for having performed the cone calorimeter tests.

## References

- [1] M. Chanda, *Plastics Technology Handbook*, 5 ed., CRC Press - Taylor&Francis Group, Boca Raton, FL, 2017
- [2] M. Bar, R. Alagirusamy, A. Das, Flame retardant polymer composites, *Fibers and Polymers*, 16 (4) (2015) 705-717. DOI: 10.1007/s12221-015-0705-6
- [3] A. Dorigato, A. Pegoretti, (Re)processing effects on linear low-density polyethylene/silica nanocomposites, *Journal of Polymer Research*, 20 (3) (2013).
- [4] D. Malpass, *Introduction to Industrial Polyethylene: Properties, Catalysts, and Processes 1ed.*, Wiley-Scrivener, 2010
- [5] G. Camino, L. Costa, M.P. Luda di Cortemiglia, Overview of Fire Retardant Mechanisms, *Polymer Degradation and Stability*, 33 (1991) 131-154.
- [6] F. Laoutid, L. Bonnaud, M. Alexandre, J.M. Lopez-Cuesta, P. Dubois, New prospects in flame retardant polymer materials: From fundamentals to nanocomposites, *Materials Science and Engineering: R: Reports*, 63 (3) (2009) 100-125. DOI: 10.1016/j.mser.2008.09.002
- [7] A. Dasari, Z.-Z. Yu, G.-P. Cai, Y.-W. Mai, Recent developments in the fire retardancy of polymeric materials, *Progress in Polymer Science*, 38 (9) (2013) 1357-1387. DOI: 10.1016/j.progpolymsci.2013.06.006
- [8] K. Aschberger, I. Campia, L.Q. Pesudo, A. Radovnikovic, V. Reina, Chemical alternatives assessment of different flame retardants – A case study including multi-walled carbon nanotubes as synergist, *Environment International*, 101 (2017) 27-45. DOI: 10.1016/j.envint.2016.12.017
- [9] S.D. Shaw, A. Blum, R. Weber, K. Kannan, D. Rich, D. Lucas, C.P. Koshland, D. Dobraca, S. Hanson, L.S. Birnbaum, Halogenated flame retardants: Do the fire safety benefits justify the risks?, *Reviews on Environmental Health*, 25 (4) (2010) 261-305.
- [10] S.L. Waaijers, D. Kong, H.S. Hendriks, C.A. de Wit, I.T. Cousins, R.H.S. Westerink, P.E.G. Leonards, M.H.S. Kraak, W. Admiraal, P. de Voogt, J.R. Parsons, Persistence, Bioaccumulation, and Toxicity of Halogen-Free Flame Retardants, in: D.M. Whitacre (ed.) *Reviews of Environmental Contamination and Toxicology*, Springer New York, New York, NY, 2013, pp. 1-71. DOI: 10.1007/978-1-4614-4717-7\_1
- [11] R.N. Rathon, P.R. Hornsby, Flame retardant effects of magnesium hydroxide, *Polymer Degradation and Stability*, 54 (2) (1996) 383-385. DOI: [https://doi.org/10.1016/S0141-3910\(96\)00067-5](https://doi.org/10.1016/S0141-3910(96)00067-5)
- [12] R. Hornsby Peter, The application of hydrated mineral fillers as fire retardant and smoke suppressing additives for polymers, *Macromolecular Symposia*, 108 (1) (2011) 203-219. DOI: 10.1002/masy.19961080117
- [13] T.R. Hull, A. Witkowski, L. Hollingbery, Fire retardant action of mineral fillers, *Polymer Degradation and Stability*, 96 (8) (2011) 1462-1469. DOI: 10.1016/j.polydegradstab.2011.05.006
- [14] M.M.Y. Zaghoul, M.M.Y. Zaghoul, Influence of flame retardant magnesium hydroxide on the mechanical properties of high density polyethylene composites, *Journal of Reinforced Plastics and Composites*, 36 (24) (2017) 1802-1816. DOI: 10.1177/0731684417727143
- [15] G.E. Zaikov, S.M. Lomakin, Ecological issue of polymer flame retardancy, *Journal of Applied Polymer Science*, 86 (10) (2002) 2449-2462. DOI: 10.1002/app.10946
- [16] F. Ren, X. Zhang, Z. Wei, J. Chen, D. Dong, X. Li, L. Zhang, Effect of particle size and content of magnesium hydroxide on flame retardant properties of asphalt, *Journal of Applied Polymer Science*, 129 (4) (2013) 2261-2272. DOI: 10.1002/app.38960
- [17] R.N. Rathon, Effects of Particulate Fillers on Flame Retardant Properties of Composites in: R.N. Rathon (ed.) *Particulate-Filled Polymer Composites*, Rapra Technology Limited, Shawbury, Shrewsbury, Shropshire, SY4 4NR, UK, 2003,
- [18] S. Kim, Flame Retardancy and Smoke Suppression of Magnesium Hydroxide Filled Polyethylene, *Journal of Polymer Science: Part B: Polymer Physics*, 41 (2003) 936-944.
- [19] G.I. Titelman, Y. Gonen, Y. Keidar, S. Bron, Discolouration of polypropylene-based compounds containing magnesium hydroxide, *Polymer Degradation and Stability*, 77 (2002) 345-352.
- [20] C.H. Hong, Y.B. Lee, J.W. Bae, J.Y. Jho, B. Uk Nam, D.-H. Chang, S.-H. Yoon, K.-J. Lee, Tensile properties and stress whitening of polypropylene/polyolefin elastomer/magnesium hydroxide flame retardant composites for cable insulating application, *Journal of Applied Polymer Science*, 97 (6) (2005) 2311-2318. DOI: 10.1002/app.21776
- [21] Z.-s. Xu, L. Yan, L. Chen, Synergistic Flame Retardant Effects between Aluminum Hydroxide and Halogen-free Flame Retardants in High Density Polyethylene Composites, *Procedia Engineering*, 135 (2016) 631-636. DOI: 10.1016/j.proeng.2016.01.130
- [22] Y. Pan, L. Han, Z. Guo, Z. Fang, Improving the flame-retardant efficiency of aluminum hydroxide with fullerene for high-density polyethylene, *Journal of Applied Polymer Science*, 134 (9) (2017). DOI: 10.1002/app.44551
- [23] Y.-Y. Yen, H.-T. Wang, W.-J. Guo, Synergistic effect of aluminum hydroxide and nanoclay on flame retardancy and mechanical properties of EPDM composites, *Journal of Applied Polymer Science*, 130 (3) (2013) 2042-2048. DOI: 10.1002/app.39394
- [24] S.-P. Liu, Flame retardant and mechanical properties of polyethylene/magnesium hydroxide/montmorillonite nanocomposites, *Journal of Industrial and Engineering Chemistry*, 20 (4) (2014) 2401-2408. DOI: 10.1016/j.jiec.2013.10.020
- [25] F. Laoutid, P. Gaudon, J.M. Taulemesse, J.M. Lopez Cuesta, J.I. Velasco, A. Piechaczyk, Study of hydromagnesite and magnesium hydroxide based fire retardant systems for ethylene-vinyl acetate containing organo-modified montmorillonite, *Polymer Degradation and Stability*, 91 (12) (2006) 3074-3082. DOI: 10.1016/j.polydegradstab.2006.08.011
- [26] L. Haurie, A.I. Fernández, J.I. Velasco, J.M. Chimenos, J.-M. Lopez Cuesta, F. Espiell, Thermal stability and flame retardancy of LDPE/EVA blends filled with synthetic hydromagnesite/aluminium hydroxide/montmorillonite and magnesium hydroxide/aluminium hydroxide/montmorillonite mixtures, *Polymer Degradation and Stability*, 92 (6) (2007) 1082-1087. DOI: 10.1016/j.polydegradstab.2007.02.014
- [27] M. Sabet, A. Hassan, C.T. Ratnam, Effect of zinc borate on flammability/thermal properties of ethylene vinyl acetate filled with metal hydroxides, *Journal of Reinforced Plastics and Composites*, 32 (15) (2013) 1122-1128. DOI: 10.1177/0731684413494942
- [28] A. Durin-France, L. Ferry, J.-M. Lopez-Cuesta, A. Crespy, Magnesium hydroxide/zinc borate/talc compositions as flame-retardants in EVA copolymer, *Polymer International*, 49 (2000)

- 1101-1105.
- [29] P.M. Visakh, Y. Arao, Flame retardants. Polymer blends, composites and nanocomposites., Springer, 2015
- [30] M. Lewin, Some comments on the modes of action of nanocomposites in the flame retardancy of polymers, *Fire and Materials*, 27 (2003) 1-7. DOI: 10.1002/fam.813
- [31] M. Lewin, Reflections on migration of clay and structural changes in nanocomposites, *Polymers for Advanced Technologies*, 17 (9-10) (2006) 758-763. DOI: 10.1002/pat.762
- [32] M. Lewin, E.M. Pearce, K. Levon, A. Mey-Marom, M. Zammarano, C.A. Wilkie, B.N. Jang, Nanocomposites at elevated temperatures: migration and structural changes, *Polymers for Advanced Technologies*, 17 (4) (2006) 226-234. DOI: 10.1002/pat.684
- [33] F. Cavodeau, B. Otazaghine, R. Sonnier, J.-M. Lopez-Cuesta, C. Delaite, Fire retardancy of ethylene-vinyl acetate composites – Evaluation of synergistic effects between ATH and diatomite fillers, *Polymer Degradation and Stability*, 129 (2016) 246-259. DOI: 10.1016/j.polymdegradstab.2016.04.018
- [34] Y. Qian, X. Zhu, S. Li, X. Chen, Flame-retardant properties of ethylene-vinyl acetate/oil sludge/ fumed silica composites, *RSC Advances*, 6 (67) (2016) 63091-63098. DOI: 10.1039/c6ra03280j
- [35] X. Chen, Y. Jiang, J. Liu, C. Jiao, Y. Qian, S. Li, Smoke suppression properties of fumed silica on flame-retardant thermoplastic polyurethane based on ammonium polyphosphate, *Journal of Thermal Analysis and Calorimetry*, 120 (3) (2015) 1493-1501. DOI: 10.1007/s10973-015-4424-4
- [36] J. Courtat, F. Melis, J.-M. Taulemesse, V. Bounor-Legare, R. Sonnier, L. Ferry, P. Cassagnau, Effect of phosphorous-modified silica on the flame retardancy of polypropylene based nanocomposites, *Polymer Degradation and Stability*, 119 (2015) 260-274. DOI: 10.1016/j.polymdegradstab.2015.05.022
- [37] M. Fu, B. Qu, Synergistic flame retardant mechanism of fumed silica in ethylene-vinyl acetate/magnesium hydroxide blends, *Polymer Degradation and Stability*, 85 (1) (2004) 633-639. DOI: 10.1016/j.polymdegradstab.2004.03.002
- [38] C.-M. Jiao, X.-L. Chen, Influence of fumed silica on the flame-retardant properties of ethylene vinyl acetate/aluminum hydroxide composites, *Journal of Applied Polymer Science*, 120 (3) (2011) 1285-1289. DOI: 10.1002/app.33126
- [39] A. Dorigato, M. D'Amato, A. Pegoretti, Effect of filler surface properties on the thermo-mechanical behaviour of high density polyethylene – fumed silica nanocomposites, *Journal of Polymer Research*, (In Press) (2011).
- [40] A. Dorigato, A. Pegoretti, A. Frache, Thermal stability of high density polyethylene–fumed silica nanocomposites, *Journal of Thermal Analysis and Calorimetry*, 109 (2) (2012) 863-873. DOI: 10.1007/s10973-012-2421-4
- [41] A. Dorigato, G. Fredi, L. Fambri, J.-M. Lopez-Cuesta, A. Pegoretti, Polyethylene-based single polymer laminates: synergistic effects of nanosilica and metal hydroxides, *Journal of reinforced plastics and composites*, 38 (2) (2018) 62-73. DOI: 10.1177/0731684418802974
- [42] M. D'Amato, A. Dorigato, L. Fambri, A. Pegoretti, High performance polyethylene nanocomposite fibers, *Express Polymer Letters*, 6 (12) (2012) 954–964.
- [43] A. Dorigato, M. D'Amato, A. Pegoretti, Thermo-mechanical properties of high density polyethylene - fumed silica nanocomposites: effect of filler surface area and treatment, *Journal of Polymer Research*, 19 (2012) 9889-9899.
- [44] A. Dorigato, A. Pegoretti, Tensile creep behaviour of poly(methylpentene)-silica nanocomposites, *Polymer International*, 59 (2010) 719-724.
- [45] A. Dorigato, A. Pegoretti, L. Fambri, M. Slouf, J. Kolarik, Cycloolefin copolymer/fumed silica nanocomposites, *Journal of Applied Polymer Science*, 119 (6) (2011) 3393-3402.
- [46] A. Dorigato, A. Pegoretti, A. Penati, Linear low-density polyethylene/silica micro- and nanocomposites: dynamic rheological measurements and modelling, *Express Polymer Letters*, 4 (2) (2010) 115-129.
- [47] A. Dorigato, M. Sebastiani, A. Pegoretti, L. Fambri, Effect of silica nanoparticles on the mechanical performances of poly(lactic acid), *Journal of Polymers and the Environment*, 20 (2012) 713–725. DOI: 10.1007/s10924-012-0425-6
- [48] V.G. Chandran, S.D. Waigaonkar, Rheological and Dynamic Mechanical Characteristics of Rotationally Moldable Linear Low-Density Polyethylene Fumed Silica Nanocomposites, *POLYMER COMPOSITES*, 37 (10) (2016) 2995-3002.
- [49] M. Batistella, B. Otazaghine, R. Sonnier, A.-S. Caro-Bretelle, C. Petter, J.-M. Lopez-Cuesta, Fire retardancy of ethylene vinyl acetate/ultrafine kaolinite composites, *Polymer Degradation and Stability*, 100 (2014) 54-62. DOI: 10.1016/j.polymdegradstab.2013.12.026
- [50] M. Batistella, B. Otazaghine, R. Sonnier, C. Petter, J.-M. Lopez-Cuesta, Fire retardancy of polypropylene/kaolinite composites, *Polymer Degradation and Stability*, 129 (2016) 260-267. DOI: 10.1016/j.polymdegradstab.2016.05.003
- [51] T. Kashiwagi, M. Mu, K. Winey, B. Cipriano, S.R. Raghavan, S. Pack, M. Rafailovich, Y. Yang, E. Grulke, J. Shields, R. Harris, J. Douglas, Relation between the viscoelastic and flammability properties of polymer nanocomposites, *Polymer*, 49 (20) (2008) 4358-4368. DOI: 10.1016/j.polymer.2008.07.054
- [52] A. Dorigato, A. Pegoretti, Fracture behaviour of linear low density polyethylene - fumed silica nanocomposites, *Engineering Fracture Mechanics*, 79 (2012) 213- 224. DOI: doi: 10.1016/j.engfracmech.2011.10.014
- [53] A. Dorigato, A. Pegoretti, J. Kolarik, Nonlinear Tensile Creep of Linear Low Density Polyethylene/Fumed Silica Nanocomposites: Time-Strain Superposition and Creep Prediction, *POLYMER COMPOSITES*, (2010) 1947-1955. DOI: <https://doi.org/10.1002/pc.20993>
- [54] C. Zhao, H. Qin, F. Gong, M. Feng, S. Zhang, M. Yang, Mechanical, thermal and flammability properties of polyethylen/clay nanocomposites, *Polymer Degradation and Stability*, 87 (2005) 183-189.
- [55] N. Garcia, M. Hoyos, J. Guzman, P. Tiemblo, Comparing the effect of nanofillers as thermal stabilizers in low density polyethylene, *Polymer Degradation and Stability*, 94 (2009) 39-48.
- [56] A. Leszczynska, J. Njuguma, K. Pielichowski, J.R. Banerjee, Polymer/montmorillonite nanocomposites with improved thermal properties. Part I. Factors influencing thermal stability and mechanisms of thermal stability improvement., *Thermochemica Acta* 453 (2007) 75–96.
- [57] A. Dorigato, L. Fambri, Effect of Aramid Regenerated Fibers on thermo-mechanical behaviour of Polyamide 12 composites, *Journal of reinforced plastics and composites*, 32 (2013) 1243-1256. DOI: 10.1177/0731684413486528
- [58] J. Gong, R. Niu, N. Tian, X.C. Chen, X. Wen, J. Liu, Z.Y. Sun, E. Mi-jowska, T. Tang, Combination of fumed silica with carbon black for simultaneously improving the thermal stability, flame retar-

dancy and mechanical properties of polyethylene, *Polymer*, 55 (13) (2014) 2998-3007.